Proceedings of the 5th International Conference on
Computation of Shell and Spatial Structures
June 1-4, 2005 Salzburg, Austria
E. Ramm, W.A. Wall, K.-U. Bletzinger, M. Bischoff (eds.)
www.iassiacm2005.de

Failure Analysis of Shear Critical RC Structural Members

Afsin Saritas, Filip C. Filippou*

*Civil and Environmental Engineering, University of California, Berkeley
filippou@ce.berkeley.edu

Abstract

This paper presents a beam finite element for the simulation of the monotonic and cyclic response of RC structural members under the interaction of flexure, axial force and shear. The proposed beam element follows the assumptions of the Timoshenko shear beam theory with a three-field Hu-Washizu variational formulation for the derivation of the element response. The nonlinear response of the element is obtained through section integration of nonlinear material response. A 3d plastic damage model for cyclic analysis of concrete is implemented with the general closest point projection algorithm. Concrete confinement effects are included by satisfaction of transverse equilibrium. The tensile and compressive response of the concrete model is related to the fracture energy, thus ensuring objectivity of numerical results. In the presence of reinforcing steel the fracture energy should be adjusted according to criteria in modern design codes.

The proposed beam element is validated by comparing the numerical response with experimental measurements of the monotonic and cyclic behavior of different type of specimens: shear deficient columns and beam, squat and slender shear walls. These correlation studies confirm the promise of the proposed approach.

1 Introduction

Extensive research on concrete material development and its application to the nonlinear analysis of RC structures has been undertaken in the last 40 years. For structural analysis in professional practice, particularly, in performance-based earthquake engineering, current studies focus on acurrate beam models, because the response of entire structures with 3d or even 2d solid finite elements is prohibitively expensive. Force-based beam elements have proven superior to displacement-based elements in the context of Euler-Bernoulli beam theory (Neuenhofer and Filippou [1]). Petrangeli, et al. [2] proposed a force-based beam element under the assumptions of the Timoshenko beam for the analysis of slender bridge piers that were flexurally dominant, but eventually failed in shear.

This paper formulates a beam element based on a three-field Hu-Washizu variational form (Taylor, et al. [3]), which exhibits the same characteristics as force-based formulations, while meeting the requirements of a more general variational framework. The nonlinear response of the element derives from the integration of nonlinear material response over the cross section. Small deformation is adopted, but large displacements are accounted for during transformation of the element response to the global reference system according to the corotational formulation. The material model is based on a 3d concrete plastic damage model (Lee and Fenves [4]) that accounts for cyclic strain histories. The effect of transverse strain on the concrete material response is included with the satisfaction of transverse force equilibrium. The numerical implementation of the material model makes use of the general closest point projection algorithm allowing for flexible incorporation within a library of plastic constitutive models in a general purpose computing environment. The tensile and compressive response of the concrete model is related to the fracture energy, thus ensuring objectivity of numerical results. In the presence of reinforcing steel the fracture energy can be adjusted according to criteria in modern design codes.

2 Finite Element Formulation

2.1 Beam Element

A beam element with a three-field Hu-Washizu functional was used for metalic shear yielding members in Saritas and Filippou [5]. We follow the same work for the beam finite element formulation. The three-field Hu-Washizu functional is expressed as

$$\Pi_{\mathrm{HW}}(\boldsymbol{\sigma},\boldsymbol{\varepsilon},\mathbf{u}) = \int_{\Omega} W(\boldsymbol{\varepsilon})\,\mathrm{d}\Omega + \int_{\Omega} \boldsymbol{\sigma}^{\mathrm{T}}\left(\boldsymbol{\varepsilon}^{\mathbf{u}} - \boldsymbol{\varepsilon}\right)\mathrm{d}\Omega + \Pi_{\mathrm{ext}} \tag{1}$$

$W(\varepsilon)$ is the strain energy function, $\boldsymbol{\varepsilon}^{\mathbf{u}}$ denotes the strains derived from displacement compatibility, and Π_{ext} is the potential energy of the external loading due to body forces, as well as displacement and traction boundary conditions. In the functional the domain of the element is denoted by Ω, the traction boundaries are denoted by Γ_{t}, and the displacement boundaries by Γ_{u}.

2.1.1 Kinematic Approximations

Limiting ourselves to the planar case, we base the displacement field $\mathbf{u}$ in (1) on the assumptions of the Timoshenko beam theory, $\mathbf{u} = \left[u_{\mathrm{x}}(x,y) \quad u_{\mathrm{y}}(x,y)\right]^{\mathrm{T}} = \left[u(x) - y\theta(x) \quad w(x)\right]^{\mathrm{T}}$, with *u(x)* the axial displacement of the beam axis, $\theta(x)$ the rotation of the beam cross section, and *w(x)* the transverse displacement of the beam axis. The compatible strains for the displacement field are obtained by differentiation: $\varepsilon_{xx}^{u} = u'(x) - y\theta'(x)$ and $\gamma_{xy}^{u} = -\theta(x) + w'(x)$. The three-field variational form offers flexibility in selecting strain fields that are independent from the displacement compatible fields. We denote these as $\varepsilon_{xx} = \varepsilon_a(x) - y\kappa(x)$ and $\gamma_{xy} = \phi(y,z)\,\gamma(x)$, where $\varepsilon_a(x)$ is the axial deformation, $\kappa(x)$ is the curvature, and $\gamma(x)$ is the shear distortion along the beam axis. The variation of the shear strain field over the cross section is described by interpolation function $\phi(y,z)$, which is derived by satisfying boundary conditions under elastostatic conditions with proper tractions on the surface of the beam.

2.1.2 Force Interpolation Functions

Taking the variation of the three-field functional in (1), and introducing the strain fields, we obtain a reduced variational form. Integration by parts of all terms with derivatives in the displacement fields reveals the suitable interpolation functions for the section forces (generalized stress terms). Moreover, this approach results in the elimination of the need for a displacement field approximation along the beam. A detailed presentation of the process is given elsewhere (Taylor, et al. [3]). The force interpolation functions are $\mathbf{s}(x) = \mathbf{b}(x)\mathbf{q} + \mathbf{s}_{\mathrm{p}}(x)$, where $\mathbf{s}(x) = \left[N(x) \quad M(x) \quad V(x)\right]^{\mathrm{T}}$ is the vector of section force resultants or generalized stresses, $\mathbf{q} = \left[q_1 \quad q_2 \quad q_3\right]^{\mathrm{T}}$ represents the independent or basic element forces, and $\mathbf{b}(x)$ is a matrix of force interpolation functions.

2.1.3 Solution of Beam Equations

After substitution of the previous matrix expressions into (1), a reduced variational form is obtained. The evaluation of the integrals along the beam axis at discrete integration points gives the matrix form of the variational functional. Subsequently, the equations are linearized at the current material state. There are three fields requiring iteration and updating: the end displacements $\overline{\mathbf{u}}$, the section deformations $\mathbf{e}$ at each integration point on the beam, and the basic element forces $\mathbf{q}$. A thorough discussion of possible solution strategies is available elsewhere (Taylor, et al. [3]) .

2.1.4 Section Model

The section forces $\mathbf{s}$ and tangent section stiffness are obtained by numerical integration of nonlinear material response over the cross section. The section model obeys the kinematics in part *2.1.1*. The strains are evaluated at each integration point, and the material model returns the corresponding stress and stiffness tensor.

2.2 Material Model

A plasticity model with small strain theory can be written as $\boldsymbol{\varepsilon} = \boldsymbol{\varepsilon}^e + \boldsymbol{\varepsilon}^p$, $\boldsymbol{\sigma} = \mathbf{E}\boldsymbol{\varepsilon}^e$, $\dot{\boldsymbol{\varepsilon}}^p = \dot{\lambda}\mathbf{m}(\boldsymbol{\sigma},\boldsymbol{\kappa})$ and $\dot{\boldsymbol{\kappa}} = \dot{\lambda}\mathbf{p}(\boldsymbol{\sigma},\boldsymbol{\kappa})$. Here $\boldsymbol{\varepsilon}$, $\boldsymbol{\varepsilon}^e$ and $\boldsymbol{\varepsilon}^p$ are the total, elastic and plastic strain tensors respectively, $\boldsymbol{\sigma}$ is the stress tensor, $\mathbf{E}$ is the elastic stiffness tensor, $\mathbf{m}$ is the flow vector, $\mathbf{p}$ are the plastic moduli, and $\boldsymbol{\kappa}$ is the set of internal variables. In a damage model, the effective stress tensor $\bar{\boldsymbol{\sigma}}$ is defined in terms of a damage parameter D, such that $\boldsymbol{\sigma} = (1-D)\bar{\boldsymbol{\sigma}}$. The plastic multiplier $\dot{\lambda}$ is determined from the Kuhn-Tucker loading/unloading conditions by replacing $\boldsymbol{\sigma}$ with $\bar{\boldsymbol{\sigma}}$: $F(\bar{\boldsymbol{\sigma}},\boldsymbol{\kappa}) \le 0$, $\dot{\lambda} \ge 0$ and $F(\bar{\boldsymbol{\sigma}},\boldsymbol{\kappa})\dot{\lambda} = 0$, where F is the yield function defining admissable stress states.

2.2.1 Constitutive Relations

In the work by Lee and Fenves [4], two damage variables, one for tensile damage D_t, and other for compressive damage D_c are defined independently. The model has two internal damage variables, $\boldsymbol{\kappa} = [\kappa_t, \kappa_c]^T$ for tension and compression. The evolution of internal variables is defined in the principal stress space as

$$\dot{\boldsymbol{\kappa}} = \dot{\lambda}\mathbf{p}(\hat{\bar{\boldsymbol{\sigma}}},\boldsymbol{\kappa}), \quad \mathbf{p} = \mathbf{h}(\hat{\bar{\boldsymbol{\sigma}}},\boldsymbol{\kappa}) \cdot \nabla_{\hat{\bar{\boldsymbol{\sigma}}}}\phi(\hat{\bar{\boldsymbol{\sigma}}},\boldsymbol{\kappa}), \quad \mathbf{h}(\hat{\bar{\boldsymbol{\sigma}}},\boldsymbol{\kappa}) = \begin{bmatrix} r(\hat{\bar{\boldsymbol{\sigma}}})\, f_t(\kappa_t)/g_t & 0 & 0 \\ 0 & 0 & (1-r(\hat{\bar{\boldsymbol{\sigma}}}))\, f_c(\kappa_c)/g_c \end{bmatrix} \tag{2}$$

A non-associative flow rule is neseccary to control the dilatancy in modeling concrete. A Drucker-Prager type function is used for the plastic potential function $\phi(\bar{\boldsymbol{\sigma}},\boldsymbol{\kappa})$ in (2), while the yield function $F(\bar{\boldsymbol{\sigma}},\boldsymbol{\kappa})$ is the Barcelona model which is a combined geometric shape from two different Drucker-Prager type functions. For a more through description of the model and its parameters see Lee and Fenves [4]. In (2) g_N *is* the specific fracture energy normalized by the characteristic length l_N where $N \in \{t,c\}$, leading to $g_N = G_N/l_N$. In order to maintain objectivity in the results, l_N should be objective. For the case of the beam element formulation, the characteristic length is selected equal to the integration weight of the corresponding section. Fracture energy in tension can be adjusted according to criteria available in design codes, as suggested by Feenstra and deBorst [6].

2.2.2 Integration of Damage Evolution Equations

The time integration of the relations with a backward Euler method results in the following residual expressions $\mathbf{R}_{\bar{\boldsymbol{\sigma}}} = \bar{\boldsymbol{\sigma}}_{n+1} + \lambda\mathbf{E}\,\mathbf{m}(\bar{\boldsymbol{\sigma}}_{n+1},\boldsymbol{\kappa}_{n+1}) - \bar{\boldsymbol{\sigma}}_{n+1}^{Trial} = \mathbf{0}$, $\mathbf{R}_{\boldsymbol{\kappa}} = \boldsymbol{\kappa}_{n+1} + \lambda\mathbf{E}\,\mathbf{m}(\bar{\boldsymbol{\sigma}}_{n+1},\boldsymbol{\kappa}_{n+1}) - \boldsymbol{\kappa}_n = \mathbf{0}$ and $\mathbf{R}_{\Delta\lambda} = F(\bar{\boldsymbol{\sigma}}_{n+1},\boldsymbol{\kappa}_{n+1}) = 0$. For the solution of these nonlinear equations, linearization is used with a iterative scheme that makes use of substepping (Perez-Foguet, et al. [7]). It is important to emphasize that the damage correction step is independent of the plastic correction steps.

2.2.3 Enforcement of Beam Dimensions from 3d Material Model

The 3d material model needs to satisfy the stress constraints of the beam problem. In the case with no transverse reinforcing steel, the plane stress conditions hold, i.e. $\sigma_y = \sigma_z = 0$. For the case with transverse reinforcement transverse equilibrium gives $\sigma_y = -\rho_{vy}\, f_{vy}$ and $\sigma_z = -\rho_{vz}\, f_{vz}$, where the transverse reinforcing ratio in the y and z directions is ρ_{vy} and ρ_{vz} and the steel stress is f_{vy} and f_{vz}, respectively. After linearization the normal strain in the y and z direction is obtained by iteration. This process accounts for the concrete confinement effect.

3 Application

The slender, shear deficient column tested by Lynn, et al. [8] demonstrates the capability of the beam formulation and the material model. The axial load on the column was 35% of the axial load capacity. The tensile and compressive fracture energies are selected as 70 N/m and 15000 N/m, respectively. The column is analyzed with one element and variable number of integration points (IP) along the beam. 10 IP are used through the section with the midpoint integration rule. The beam element does not suffer from shear locking. The results in Fig. 1 show convergence upon mesh refinement with objectivity of the response under softening material conditions and good agreement with the measured cyclic envelope of the hysteretic column response. At least 4 IP are required for accuracy. Further refinement does not lead to significant improvement. Further calibration of material parameters is necessary and a more extensive set of validation studies is in progress.

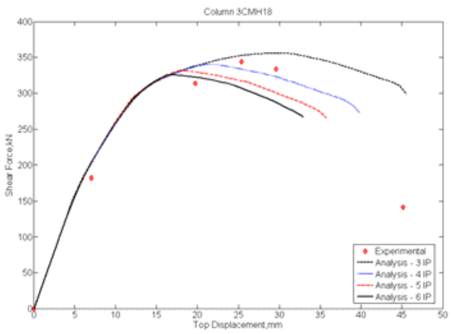

Figure 1 Load – Deformation Response

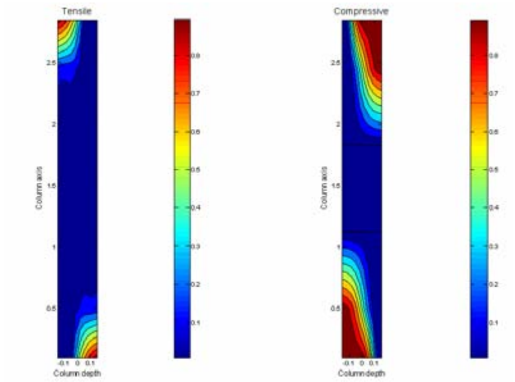

Figure 2 Damage Disttribution

4 Conclusion

The proposed beam element with the 3d concrete plastic damage model shows considerable promise. The overall response of various RC member types is captured well, while equally satisfactory agreement is obtained with local response measures, such as measured internal strain distributions and visible damage. Thorough identification of material parameters and validation studies with various concrete specimens are in progress.

References

[1] A. Neuenhofer, and F.C. Filippou, "Evaluation of Nonlinear Frame Finite Element Models," *Journal of Structural Engineering, ASCE*, Vol. 123, pp. 958-966, 1997.

[2] M. Petrangeli, P. E. Pinto, and V. Ciampi, "Fiber element for cyclic bending and shear of RC structures. I: Theory," *Journal of Engineering Mechanics-Asce*, vol. 125, pp. 994-1001, 1999.

[3] R. L. Taylor, F. C. Filippou, A. Saritas, and F. Auricchio, "Mixed finite element method for beam and frame problems," *Computational Mechanics*, vol. 31, pp. 192-203, 2003.

[4] J. Lee and G. L. Fenves, "Plastic-damage Model for Cyclic Loading of Concrete Structures," *Journal of Engineering Mechanics, ASCE*, vol. 124, pp. 892-900, 1998.

[5] A. Saritas and F. C. Filippou, "Modeling of Shear Yielding Members for Seismic Energy Dissipation," presented at 13th World Conference on Earthquake Engineering, Vancouver, BC Canada, 2004.

[6] P. H. Feenstra and R. De Borst, "Constitutive Model for Reinforced Concrete," *Journal of Engineering Mechanics, ASCE*, vol. 121, pp. 587-595, 1995.

[7] A. Perez-Foguet, A. Rodriguez-Ferran, and A. Huerta, "Consistent tangent matrices for substepping schemes," *Computer Methods in Applied Mechanics and Engineering*, vol. 190, pp. 4627-4647, 2001.

[8] A. C. Lynn, J. P. Moehle, S. A. Mahin, and W. T. Holmes, "Seismic Evaluation of Existing Reinforced Concrete Building Columns," *Earthquake Spectra*, vol. 12, pp. 715-739, 1996.